

RESEARCH ARTICLE

# Splice donor site sgRNAs enhance CRISPR/Cas9-mediated knockout efficiency

Ignacio García-Tuñón <sup>1,2</sup>, Verónica Alonso-Pérez <sup>1,2</sup>, Elena Vuelta <sup>3</sup>, Sandra Pérez-Ramos<sup>3</sup>, María Herrero <sup>3</sup>, Lucía Méndez<sup>3</sup>, Jesús María Hernández-Sánchez <sup>1,2</sup>, Marta Martín-Izquierdo<sup>1,2</sup>, Raquel Saldaña<sup>4</sup>, Julián Sevilla <sup>5</sup>, Fermín Sánchez-Guijo<sup>1,2,6</sup>, Jesús María Hernández-Rivas<sup>1,2,6</sup>, Manuel Sánchez-Martín <sup>2,3,7</sup>\*

1 Unidad de Diagnóstico Molecular y Celular del Cáncer, Centro de Investigación del Cáncer-IBMCC (USAL-CSIC), Salamanca, Spain, 2 IBSAL, Instituto de Investigación Biomédica de Salamanca, Salamanca, Spain, 3 Servicio de Transgénesis, Nucleus, Universidad de Salamanca, Salamanca, Spain, 4 Servicio de Hematología, Hospital de Especialidades de Jerez, Zacatecas, Spain, 5 Hospital Infantil Universitario Niño Jesús, Madrid, Spain, 6 Servicio de Hematología, Hospital Universitario de Salamanca, Salamanca, Spain, 7 Departamento de Medicina, Universidad de Salamanca, Salamanca, Spain

 These authors contributed equally to this work.

\* [adolsan@usal.es](mailto:adolsan@usal.es)



 OPEN ACCESS

**Citation:** García-Tuñón I, Alonso-Pérez V, Vuelta E, Pérez-Ramos S, Herrero M, Méndez L, et al. (2019) Splice donor site sgRNAs enhance CRISPR/Cas9-mediated knockout efficiency. PLoS ONE 14 (5): e0216674. <https://doi.org/10.1371/journal.pone.0216674>

**Editor:** Stefan Maas, National Institutes of Health, UNITED STATES

**Received:** February 7, 2019

**Accepted:** April 26, 2019

**Published:** May 9, 2019

**Copyright:** © 2019 García-Tuñón et al. This is an open access article distributed under the terms of the [Creative Commons Attribution License](https://creativecommons.org/licenses/by/4.0/), which permits unrestricted use, distribution, and reproduction in any medium, provided the original author and source are credited.

**Data Availability Statement:** All relevant data are within the manuscript and its Supporting Information files.

**Funding:** This work was mainly supported by a grant from the Fondo de Investigaciones Sanitarias (FIS) of the Spanish Ministry of Economy and Competitiveness and the European Regional Development Fund (ERDF) “Una manera de hacer Europa” [grant PI17/01895 to IGT and MSM.]; Junta de Castilla y León, Fondos FEDER [SA085U16 to JMHR]; Novartis grant; and by the

## Abstract

CRISPR/Cas9 allows the generation of knockout cell lines and null zygotes by inducing site-specific double-stranded breaks. In most cases the DSB is repaired by non-homologous end joining, resulting in small nucleotide insertions or deletions that can be used to construct knockout alleles. However, these mutations do not produce the desired null result in all cases, but instead generate a similar, functionally active protein. This effect could limit the therapeutic efficiency of gene therapy strategies based on abrogating oncogene expression, and therefore needs to be considered carefully. If there is an acceptable degree of efficiency of CRISPR/Cas9 delivery to cells, the key step for success lies in the effectiveness of a specific sgRNA at knocking out the oncogene, when only one sgRNA can be used. This study shows that the null effect could be increased with an sgRNA targeting the splice donor site (SDS) of the chosen exon. Following this strategy, the generation of null alleles would be facilitated in two independent ways: the probability of producing a frameshift mutation and the probability of interrupting the canonical mechanism of pre-mRNA splicing. In these contexts, we propose to improve the loss-of-function yield driving the CRISPR system at the SDS of critical exons.

## Introduction

With the recent diversification of genome editing tools, including those involving clustered, regularly interspaced short palindromic repeats and their nuclease-associated protein Cas9 (CRISPR/Cas9), the landscape of suppression techniques has dramatically changed. Although CRISPR/Cas9 is similar in action and efficacy to protein-based targeted nucleases, such as zinc finger nucleases (ZFNs) and transcription activator-like effector nucleases (TALENs)[1], the ease with which these reagents can be designed and tested through the construction of single-

Fundación “Jabones para Daniel”. JM Hernández-Sánchez was supported by a research grant from Fundación Española de Hematología y Hemoterapia (FEHH). The funders had no role in study design, data collection and analysis, decision to publish, or preparation of the manuscript.

**Competing interests:** The authors have declared that no competing interests exist.

guide RNAs (sgRNAs) has made gene editing available to a wider variety of users and for a broader range of applications. Unlike ribozymes, antisense oligodeoxynucleotides (AS-ODNs) and short interfering RNAs (siRNAs), CRISPR/Cas9 works at the DNA level, where it has the advantage of providing permanent and full gene knockout, while other methods only silence genes transiently[2,3]. CRISPR/Cas9 cuts DNA in a sequence-specific manner with the possibility of interrupting coding sequences, thereby making it possible to turn off cancer drivers in a way that was not previously feasible in humans[4,5]. This notable application of permanent gene disruption is based on the cellular mechanisms involved in double-stranded break (DSB) repair. Nonhomologous DNA end-joining (NHEJ) is the predominant DSB repair pathway throughout the cell cycle. Following the creation of a DSB within the coding sequence of a gene, the predominant and error-prone NHEJ pathway often results in small nucleotide insertions or deletions (indels)[6]. Its great efficiency at inducing DSB has led to CRISPR/Cas9 technology gaining a reputation as the gold standard for creating null alleles *in vivo* and *in vitro*. These null alleles can arise from NHEJ indels that trigger premature stop codons (frame-shift mutation) and/or non-sense-mediated decay in the target gene, resulting in loss of function. Currently, CRISPR/Cas9 is extensively used to engineer gene knockouts in most biological systems, but due to the variable size of the NHEJ-induced indel, it is not always possible to generate a full KO in one step. When the delivery of Cas9 elements is effective, full KO generation requires off-frame mutations in both alleles, which is a matter of probability since the random nature of DNA repair gives rise to considerable heterogeneity within the cell. It entails dealing with a significant frequency of mutated cells in which the outcome of mutation could preserve the reading frame (i.e., +3 or -3 mutations)[7]. A possible solution is to use two or more RNA guides to knock out the gene at several key sites in an attempt to guarantee the null result. However, a high proportion of off-targets would increase with each new sgRNA added. Conversely, more sgRNAs at the same time trigger more DSBs, which induces a stronger p53-mediated DNA damage response[8] and more complex rearrangements[9]. Either way, these undesirable effects may be irrelevant in assays in which the knockout cell can be sequenced, selected and expanded, or the null allele of the animal model can be segregated. Nevertheless, there are other situations, either *in vivo* or *in vitro*, in which cell selection and clone expansion are not available, and achieving high levels of knockout or gene inactivation efficiency is crucial[10,11]. Thus, it is important to study the key exons carefully and, more importantly, the target areas inside them, before making a selection[12]. Hematological cancer therapies based on specific oncogenic silencing within primitive pluripotent stem cells may be the best example of these situations. In this pathological cell context, the highly efficient interruption of the oncogenic open reading frame (ORF) might be an effective therapeutic option. It would even be more important for those tumors directed by a single oncogenic event, as is the case for several leukemias or sarcomas, which are directed by specific fusion oncoproteins [13,14]. A recent study of the *BCR/ABL* oncogene showed this gene fusion to be an ideal target for CRISPR/Cas9-mediated gene therapy. A CRISPR-Cas9 application truncated the specific *BCR-ABL* fusion (p210) abrogating its oncogenic potential, but to achieve *in vivo* effectiveness in a xenograft model, the authors had to select and expand the correctly edited cellular clone because some of the clones contained in-frame or non-synonymous mutations[5,15]. Therefore, in these situations, it is essential to have not only highly efficient Cas9-sgRNA cell delivery, but also a high capacity for generating null mutations. This is especially critical for cancer oncogene suppression therapies based on disrupting driver oncogenes. If the efficiency of CRISPR/Cas9 reagent delivery to the cancer cell is acceptable, the key step to success lies in the effectiveness with which a specific sgRNA can knock out the oncogene. In this way, for most knockout studies in which the edited cells or mice can be selected, the sgRNA targets different positions within the chosen exon, avoiding exon boundaries. In most of these cases, the

sgRNA design follows only off-target criteria, but for cases in which cellular selection is not an option and only one sgRNA can be used, the null effect could be strengthened with an sgRNA that targets splice site consensus sequences or close to them. Following this strategy, the generation of null alleles would be enhanced in two ways: by producing a frameshift mutation and by breaking the canonical mechanism of pre-mRNA splicing. In this sense, it has long been known that mutations in splice-site consensus sequences can affect pre-mRNA splicing patterns and can lead to the generation of null or deficient alleles[16]. In fact, pioneering genetic studies indicated that many of the thalassemia mutations in the  $\beta$ -globin gene affect splice sites and give rise to aberrant splicing patterns[17,18]. Recent studies have demonstrated that a splicing mutation in the STAR gene is a loss-of-function mutation that produces an aberrant protein[19]. Nonsense-mediated mRNA decay (NMD), a conserved biological mechanism that degrades transcripts containing premature translation termination codons, could help secure the null effect when a DSB is induced at splice sites. In addition to transcripts derived from nonsense alleles, the substrates of the NMD pathway include pre-mRNAs that enter the cytoplasm with their introns intact[20]. Several mutations of splice donor sites that cause loss of gene function have recently been identified. A novel mutation at a splice donor site that was predicted to lead to skipping of exon 10 of the PLA2G6 gene was found in a homozygous state in infantile neuroaxonal dystrophy patients. This variant has been correlated with loss of function, providing further evidence of its pathogenicity[21]. Mutations in the ectodysplasin A1 gene (EDA-A1) at the splice donor site have been described in patients with hypohydrotic ectodermal dysplasia. This novel functional skipping-splicing EDA mutation was the cause of the pathological phenotype[22]. Studies in a family with premature ovarian failure identified a variant that alters a splice donor site. This variant resulted in a predicted loss of function of the MCM9 gene, which is involved in homologous recombination and repair of double-stranded DNA breaks[23].

Taking into account all these findings, we decided to explore the effectiveness of driving one single sgRNA targeting the splice-donor exon site (SDE-sgRNA) to increase the null allele yield. To compare the knockout efficiency of SDE-sgRNAs and sgRNAs targeting positions within the exon (IE-sgRNA) we induced DSB with both guides in critical exons in three genes (*TYR*, *ATM* and *ABL*), two systems (*in vivo* and *in vitro*), and two species (human and mouse). Finally, we sequenced all mutant alleles generated and analyzed the consequences *in silico* and *in vivo*.

## Results

### The sgRNA guides targeting splice-donor sites of key exons increase the generation *in vitro* and *in vivo* of null alleles in mouse and human cells

***In vitro.*** Two groups of sgRNAs were created to study the efficiency of SDE-sgRNAs and IE-sgRNAs at generating null alleles in mouse and human cells (Fig 1). All guides were designed to target the Tyrosinase, and *ATM* genes in both species in key exons.

Three individual electroporation assays were performed with each sgRNA in Baf/3 mouse cells and K562 human cells. Mouse *Tyr* exon 1, mouse *ATM* exon 10, human *Tyr* exon1 and human *ATM* exon10 sgRNAs (SDE-sgRNA and IE-sgRNA for each one) were cloned in a CRISPR-Cas9-GFP mammalian expression vector. An empty CRISPR-Cas9-GFP vector was used as a control. GFP expression was detectable 24 hours post-electroporation in all cases, indicating the effective delivery of the CRISPR/Cas9 system and its expression in Baf/3 or K562 cells (Fig 2A). GFP+ cells were sorted and subjected to Sanger sequencing, which revealed no variations in the target sequence of control cells. Sanger sequencing identified indel mutations at the predicted cleavage point in CRISPR/Cas9 assays, while no sequence

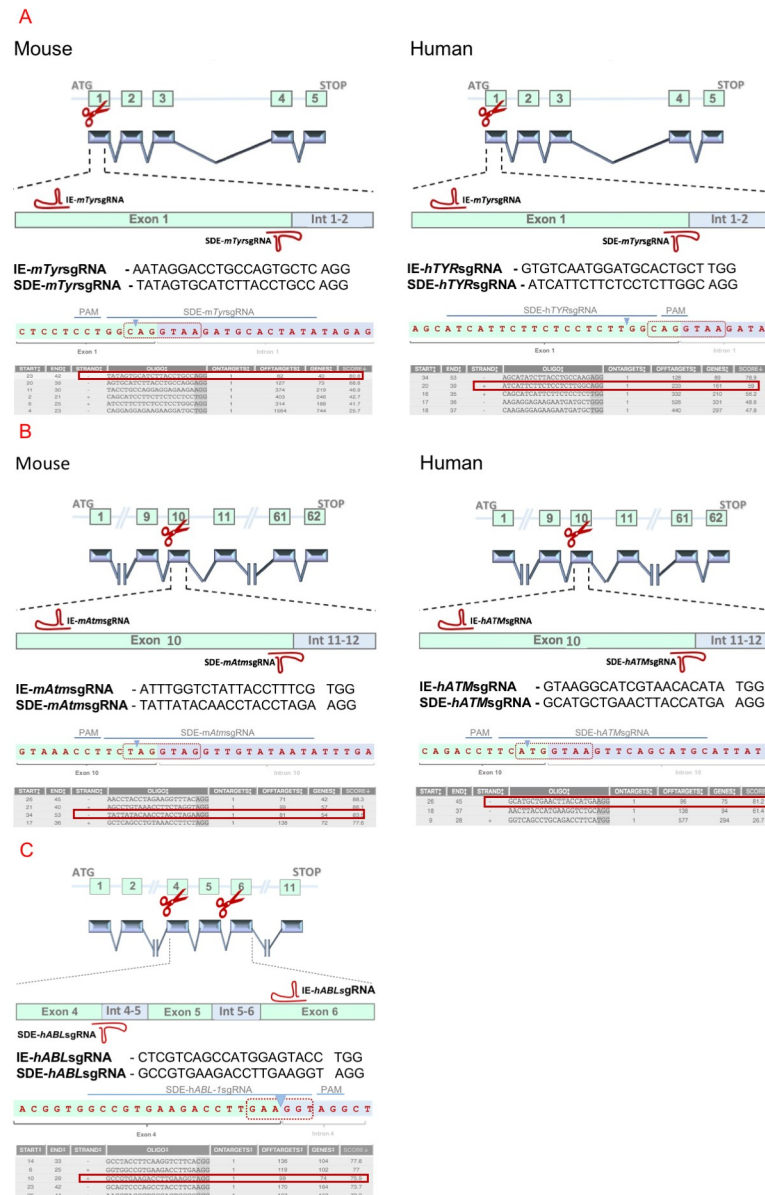


**Fig 1. Experimental design of genome editing of TYR, ATM and ABL-1 loci by CRISPR/Cas9 system.** (A) Schematic representation of the mouse and human *Tyr* loci and the CRISPR/Cas9 experimental design of the two RNA guides are represented in the exon 1 sequence. SDE-sgRNAs match the splice site between exon 1 and intron 1–2. IE-sgRNAs target a central position at the coding sequence of exon 1. (B) Schematic representation of the mouse and human *ATM* loci and the CRISPR/Cas9 experimental design of the two RNA guides are represented in the exon 10 sequence. SDE-sgRNAs match the splice site between exon 10 and intron 10–11, and IE-sgRNAs target a coding sequence of exon 10. (C) Schematic representation of the human *ABL-1* locus and the CRISPR/Cas9 experimental design of the two RNA guides. SDE-sgRNAs match the splice site between exon 4 and intron 4–5, and IE-sgRNAs target a coding sequence of exon 6. Sequences of each SDE-sgRNA are represented (blue line) and its expected cleavage point (blue arrowhead) at the splice donor sequence (red dotted box). Also, several candidates to SDE-sgRNAs are listed with its respective scores (red box correspond to selected sgRNAs).

<https://doi.org/10.1371/journal.pone.0216674.g001>

variations were observed in control cells (Fig 2B). Tracking of indels by decomposition (TIDE) analysis showed similar overall DSB-induced efficiency between SDE-sgRNA and IE-sgRNA in the Baf/3 or K562 cell lines. In knockout assays with both sgRNAs, the TIDE algorithm of Baf/3 and K562 mutant cells predicted small deletions (1–7 bp) in most cases (Fig 3).

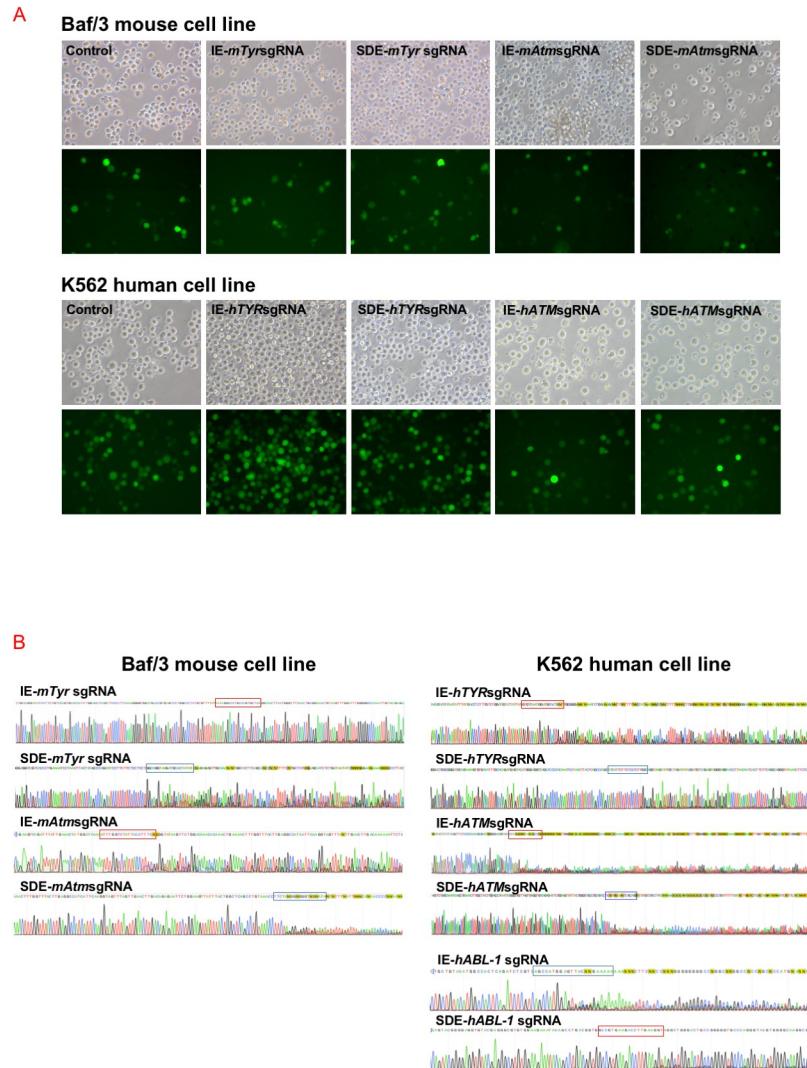


**Fig 2. *In vitro* CRISPR/Cas9-mediated edition of *Tyr* and *Atm* loci in the Baf/3 mouse cell line, and *TYR*, *ATM* and *ABL-1* in the K562 human cell line.** (A) Fluorescent microscopy of cells electroporated with empty px480 vector (controls) and carrying each RNA guides. (B) Sequences of CRISPR/Cas9 edited cells through IE-sgRNA (red box) and SDE-sgRNA (blue box). Edited cells showed a mixture of sequences around the expected cleavage point for each sgRNA.

<https://doi.org/10.1371/journal.pone.0216674.g002>

To eliminate interference in Cas9 delivery efficiency among assays, we decided to analyze only the mutant alleles generated by every guide and their consequences for the obviation of wildtype or well-repaired alleles. In order to gain detailed information about all mutant alleles for each sgRNA we analyzed the genome of properly electroporated Baf/3 or k562 cells by next-generation sequencing (NGS) (S1–S4 Tables). Unlike with the Sanger analysis, NGS revealed a high number of mutated alleles in both groups. Several of detected alleles shown in-frame indels that deleted 1–6 amino acids, thereby preserving the reading frame of the protein (S1–S4 Tables). However, *in silico* analysis of the allelic modifications generated by SDE-sgRNA predict the generation of a null allele in all cases, by frameshift mutations or by loss of canonical splicing sequences, or both simultaneously (Fig 4).

In order to evaluate the functionality of the mutant alleles generated by the CRISPR/Cas9 system in the human *ATM* gene, protein levels in K562-edited cells were analyzed by western

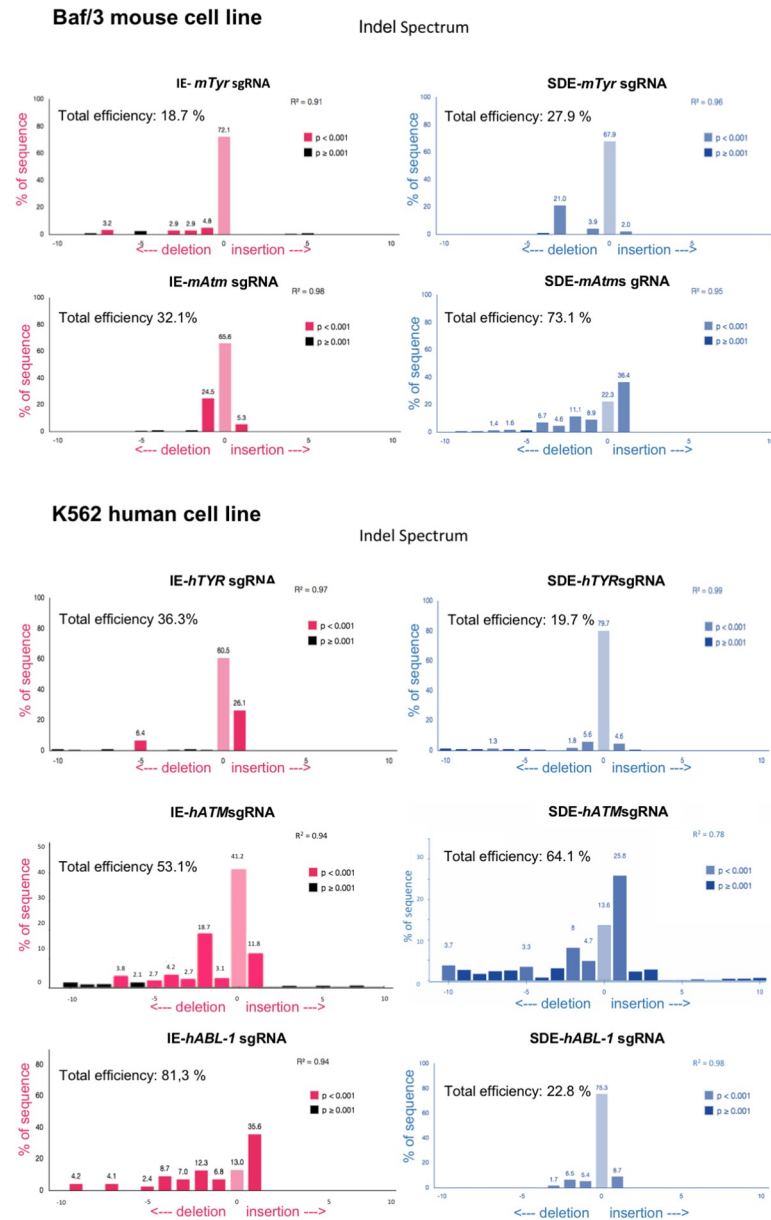


**Fig 3. TIDE decomposition analysis of edited sequences generated in human and mouse cell lines.** TIDE decomposition algorithm prediction of the overall edition efficacy and most common allele variations generated for IE-sgRNAs (red panels) and for SDE-sg-RNAs (blue panels).

<https://doi.org/10.1371/journal.pone.0216674.g003>

blot (WB). While IE-*hATM*sgRNA-transfected cells showed slightly weaker *ATM* expression compared with K562 parental cells, low levels of *ATM* protein were detected in SDE-*hATM*sgRNA-transfected cells (Fig 5A). Single-cell-derived cell lines from both IE-*hATM*sgRNA (6 clones) and SDE-*hATM*sgRNA-SD (6 clones) K562 cells were established and analyzed by NGS (S5 Table). *ATM* protein levels of each single-cell-derived clone were analyzed by WB. Most mutated cell clones (4/6) edited with IE-*hATM*sgRNA showed *ATM* expression (Fig 5B). NGS analysis of all single-cell clones edited with IE-*hATM*sgRNA had at least one functional allele, either a wildtype (wt) or with in-frame mutations (S5 Table). However, several mutated cell clones (5/6) edited with SDE-*hATM*sgRNA had no levels of *ATM*

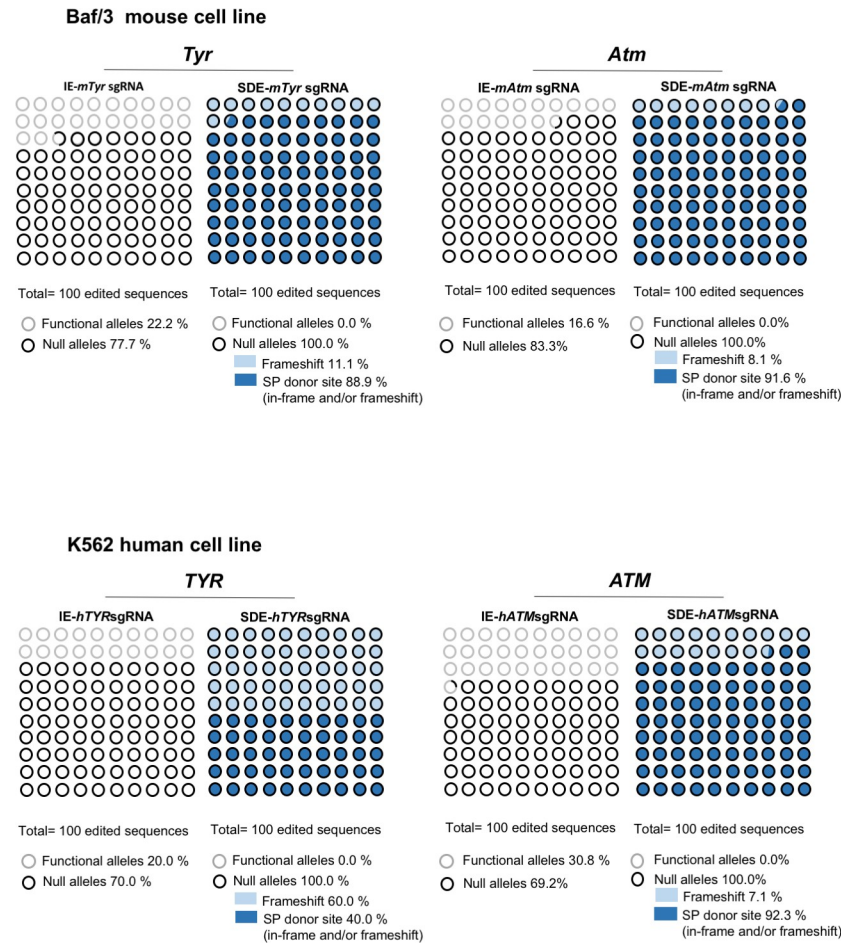


**Fig 4. Next Generation Sequencing (NGS) analysis of *TYR* and *ATM* genes in mouse and human edited cells.** Graphic representation of the mutations found in edited cells by IE-sgRNA and SDE-sgRNA, and their predicted effect. Black and gray circles represent null alleles and functional alleles respectively, while the background indicates the type of mutation (dark blue: splice donor site in-frame and/or frameshift; light blue: frameshift).

<https://doi.org/10.1371/journal.pone.0216674.g004>

protein that could be detected by WB (Fig 5B). Analyzing them showed splicing mutations together with in-frame or frameshift mutations in both *ATM* alleles (S5 Table).

**In vivo.** One-cell stage embryos from two strains of mice, inbred C57Bl6/J and F2 hybrids of B6/CBA, were microinjected with Cas9 mRNA and *Tyr* sgRNAs. No nucleotide polymorphisms between C57Bl6/J and CBA strains at *Tyr* exon1/intron1 were found. The microinjected embryos were divided in two groups, one of which was grown to blast stage and harvested to obtain the genomic DNA, which was analyzed to detect indels at the sgRNA cut-sites. Embryos of the other group were grown to the two-cell stage and implanted in pseudo-pregnant females to visualize the *in vivo* CRISPR effect on mouse coat color. The microinjected zygotes grown to blast stage were harvested to obtain their genomic DNA, which was then analyzed by NGS, revealing a greater abundance of null alleles in the SDE-*mTyr*sgRNA than in the IE-*mTyr*sgRNA embryo group (100% vs. 67.57%) (S6 Table). Briefly, NGS detected seven mutated alleles at the expected cut-site of IE-*mTyr*sgRNA. *In silico* analysis identified three mutated alleles with in-frame mutations that gave rise to a putative functional protein. NGS in the group of embryos microinjected with SDE-*mTyr*sgRNA identified eight mutated alleles, of which three were in-frame mutations and five were null mutations. However, in this embryo

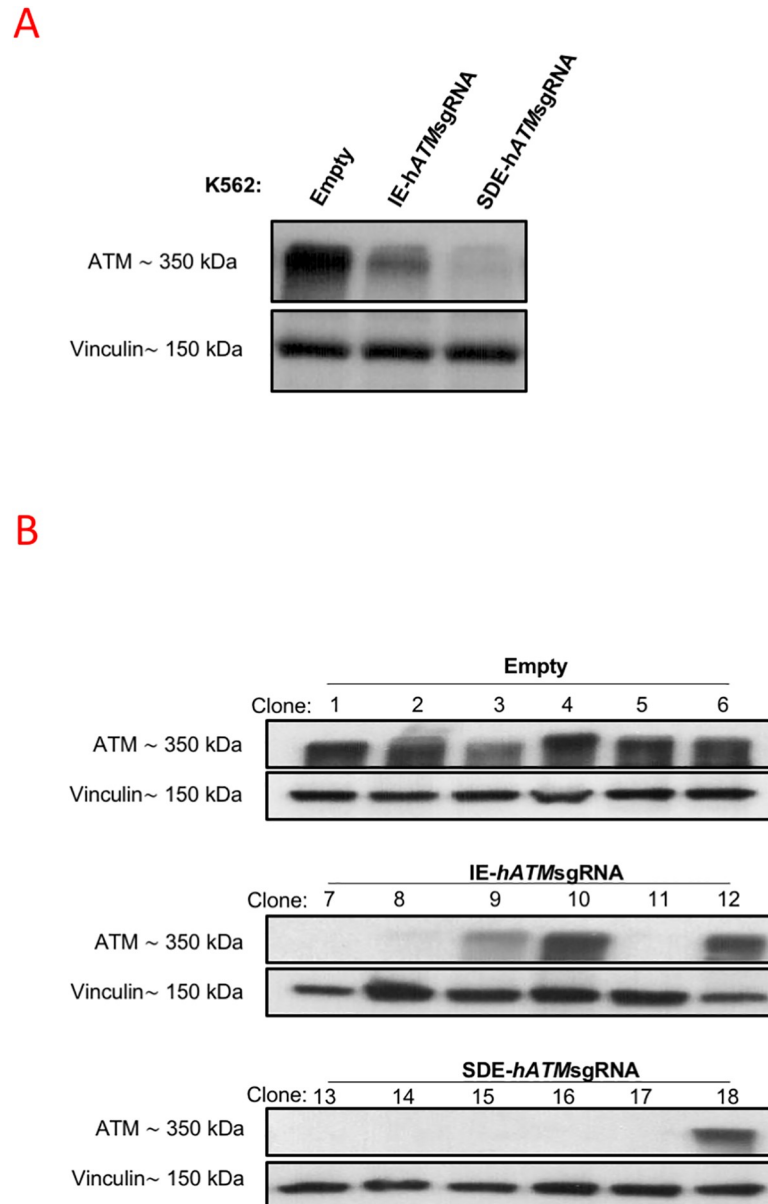


**Fig 5. Analysis of ATM gene expression by Western blot in K562 edited cells.** (A) Western blot analysis of ATM protein expression in K562-edited cells. A single band of 350 kDa corresponding to ATM was observed in K562 cells electroporated with empty px458. A lower level of ATM expression was observed in IE-hATMsgRNA-edited cells, and an even lower level was noted in SDE-hATMsgRNA-edited cells. Vinculin expression of the cells was used as the loading control. (B) Western blot analysis of ATM expression in single-edited-cell clones. All clones derived from cells electroporated with empty vector, used as a control, showed a single band corresponding to ATM. Three of six IE-hATMsgRNA edited clones showed no expression of ATM and one of six had a lower level of ATM expression compared with controls. Only one of six SDE-hATMsgRNA-edited clones expressed ATM, while ATM expression could not be detected in the other five clones.

<https://doi.org/10.1371/journal.pone.0216674.g005>

group, all alleles (100%) detected were predicted to be null alleles given the splicing site mutations (Fig 6 and S6 Table).

To confirm the *in-silico* predictions, one-cell stage embryos from two strains of mice were microinjected with Cas9 mRNA and both Tyr sgRNAs separately. Embryos microinjected with SDE-*mTyrsgRNA* or IE-*mTyrsgRNA* were implanted in two cell-stage in pseudopregnant

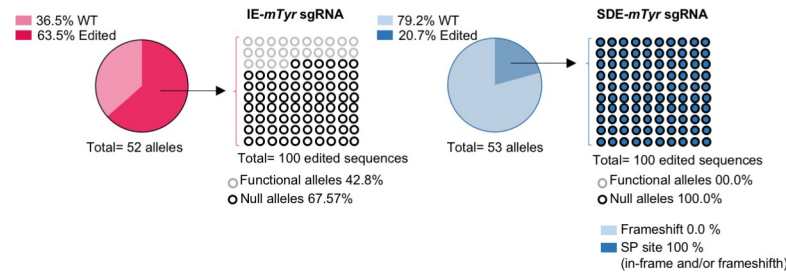


**Fig 6. Next Generation Sequencing (NGS) analysis of CRISPR/Cas9 edited mouse embryos at *Tyr* locus.** Graphic NGS analysis of CRISPR/Cas9-mediated edition of *Tyr* locus in mouse blastocysts. Genotyping of embryos microinjected with sgRNAs targeting *Tyr* gene, by NGS, revealed that only 67.57% of edited sequences from embryos microinjected with IE-*mTyr*sgRNA correspond to null alleles, while 100% SDE-*mTyr*sgRNA-modified alleles gave rise to null alleles. Black and gray circles correspond to null and functional alleles, respectively, while the background indicates the type of mutation (dark blue: splice donor site in-frame and/or frameshift; light blue: frameshift).

<https://doi.org/10.1371/journal.pone.0216674.g006>

females. Full albinos, mosaics, and colored-coat pups were detected in all offspring of each group of microinjected embryos in both strains (Fig 7). 60 mice per group were analyzed by Sanger sequencing and a large number of mutant mice with one or two mutant alleles were detected. To address which sgRNA yielded a higher proportion of null alleles, we excluded all mice with unmuted alleles. All mice with at least one mutant allele (mosaic mice) were analyzed *in silico*. We detected a higher number of albino or mosaic mice in the SDE-*mTyr*sgRNA mouse group compared with the IE-*mTyr*sgRNA group (S7 Table).

Sanger sequencing and TIDE analysis of the SDE-*mTyr*sgRNA mouse group with any grade of albinism identified at least two alleles with frameshift mutations and/or splice mutations. As a representative example we show an offspring where we detected mosaic pups with three alleles: a wildtype allele, a frameshift null allele and a splicing-site-mutated allele arising from a point mutation (+1 bp insertion) at the intronic splice-site. We also detected coat-colored pups in IE-*mTyr*sgRNA targeted pups exclusively with two mutated alleles: a frameshift allele and a mutated allele arising from a nonsynonymous mutation (Fig 7 and S7 Table).

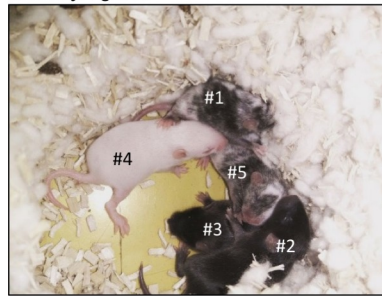
### The sgRNA guide targeting the exon splice-donor site of *BCR/ABL* oncogene increases the efficiency for abrogating cell survival / proliferation oncogen-dependent

To test the efficiency of SDE-sgRNA and IE-sgRNA guides at switching off oncogenes we performed similar assays to generate *ABL* null alleles in the leukemic K562 cell line and to abrogate the oncogene activity of *BCR/ABL* oncogene fusion (Fig 1C).

Similarly to *TYR* and *ATM* genes, three individual electroporation assays of K562 cells were performed with each sgRNA directed towards the *ABL* exon 1 (SDE-*hABL-1*sgRNA and IE-*hABL-1*sgRNA) cloned in a CRISPR-Cas9-GFP mammalian expression vector. Sanger sequencing showed genome edition at expected cleavage point for each sgRNA guide and Tide analysis predicted a variety of small indels for each guide (Figs 2 and 3). NGS analysis showed the most frequent allele variations generated in K562 by electroporation with SDE- and IE-*hABL-1* sgRNAs (S8 Table). 40% (4/10) of the allelic variations generated by IE-*hABL-1* sgRNA gave rise to in-frame mutations. By contrast, SDE-*hABL-1* sgRNA gave rise to 100% (9/9) of knockout sequences, four of which (44.4%) were in-frame mutations, but with an altered canonical splicing sequence (S8 Table).

To test the ability of SDE sgRNAs to increase the efficiency at knocking out fusion oncogenes, we compared the proficiency at abrogating the cell survival and proliferation produced

SDE-mTyr sgRNA



SDE-mTYRsgRNA	Sequence (Splice site; Exon; Intron)	Mutation	Result	Protein translation
WT	AGCCGAGTCCTCTTCTCTCTGGCAGGTAAAGATGCACATATAGAG			
<b>Mosaic # 1</b>	WT AGCCGAGTCCTCTTCTCTCTGGCAGGTAAAGATGCACATATAGAG Del CAGGTA AGCCGAGTCCTCTTCTCTCTGGCAGGTAAAGATGCACATATAGAG	In frame -3 bp / Sp donor site -6 bp	QI-	Yes
	Del G AGCCGAGTCCTCTTCTCTCTGGCAGGTAAAGATGCACATATAGAG	Sp donor site -2bp		No
<b>Black # 2</b>	WT AGCCGAGTCCTCTTCTCTCTGGCAGGTAAAGATGCACATATAGAG			Yes
<b>Mosaic # 3</b>	WT AGCCGAGTCCTCTTCTCTCTGGCAGGTAAAGATGCACATATAGAG Del GGTA AGCCGAGTCCTCTTCTCTCTGGCAAGGTAAAGATGCACATATAGAG Ins A AGCCGAGTCCTCTTCTCTCTGGCAAGGTAAAGATGCACATATAGAG	Frameshift -1 bp / Sp donor site -5 bp Frameshift +1 bp / Sp donor site +1 bp		No No
<b>Mosaic # 4</b>	WT AGCCGAGTCCTCTTCTCTCTGGCAGGTAAAGATGCACATATAGAG Del CAGGTAAG AGCCGAGTCCTCTTCTCTCTGGCAAGGTAAAGATGCACATATAGAG Del GG / Ins CAT AGCCGAGTCCTCTTCTCTCTGGCAGGTAAAGATGCACATATAGAG	In frame -3 bp / Sp donor site -7 bp Sp donor site	QI-	No No
<b>Albino # 5</b>	Del A AGCCGAGTCCTCTTCTCTCTGGCAGGTAAAGATGCACATATAGAG Del CCTGGCAGGTA / Ins ATAT AGCCGAGTCCTCTTCTCTATATAAGATGCACATATAGAG	Frameshift -1 bp / Sp donor site -1bp In frame / Sp donor site		No No

**Fig 7. In vivo Analysis of Tyr-null alleles generation by CRISPR/Cas9-induced mutations.** A representative off-spring obtained from SDE-mTyrsgRNA. Most pups of SDE-mTyrsgRNA -edited embryos (4 of 5) showed a mutant phenotype (1 albino and 3 mosaic). The genetic characterization of the different alleles of the off-spring is showed below.

<https://doi.org/10.1371/journal.pone.0216674.g007>

by the *BCR-ABL* oncoprotein through the induction of indels with SDE-sgRNA and IE-sgRNA CRISPR-Cas9 guides. In three independent assays, we electroporated the K562 *BCR/ABL* cell line with SDE-*hABL-1* and IE-*hABL-1*sgRNA. After 48 hours, we analyzed the effects on apoptosis and cell cycle (Fig 8). SDE-*hABL-1*sgRNA-targeted cells showed a higher level of apoptosis (86.8%) than noted in IE-*hABL-1*sgRNA cells (60.1%), while 32.4% of control cells were apoptotic (Fig 8A). K562 cells electroporated with SDE sgRNA yielded 10% more subG0 DNA content (45.3%) than IE-edited cells (34.5%) (Fig 8B). The quantification of annexin expression in K562-edited cells with SDE- and IE-*hABL-1* sgRNAs showed a higher level of expression in SDE-*hABL-1*sgRNA-edited cells (568.2 mfi) compared with IE-*hABL-1*sgRNA-edited cells (475.5 mfi) and K562 control cells (411.5 mfi) (Fig 8C).

### Off-targets analysis showed no differences between sgRNAs designed against splice-donor site and internal-exon region

To determinate if the predicted off-targets were affected in a major manner by the SDE sgRNAs we studied the top 5 predicted off-targets of each independent sgRNA (Fig 9). We tested the ability of each sgRNA to induce genome edition in off-target sequences by the observation the heteroduplex formed in the edited sequences. The IE-sgRNAs produced genome edition in 5 of 25 analyzed off-target sequences, and the same proportion of edited off-target was found in SDE-sgRNAs, producing 4 altered sequences of 25 (Fig 9). Statistical analysis showed no significant differences between both sgRNAs groups (p value = 0.751).

### Discussion

DSB induced by CRISPR/Cas9 technology is the gold standard for creating null alleles in any biological system. In most cases, DSBs are typically repaired by NHEJ, resulting in indel

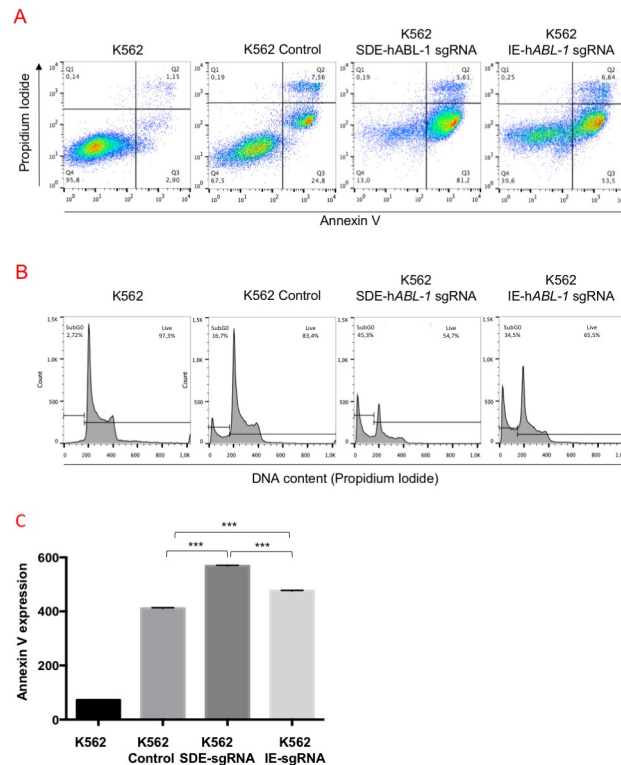
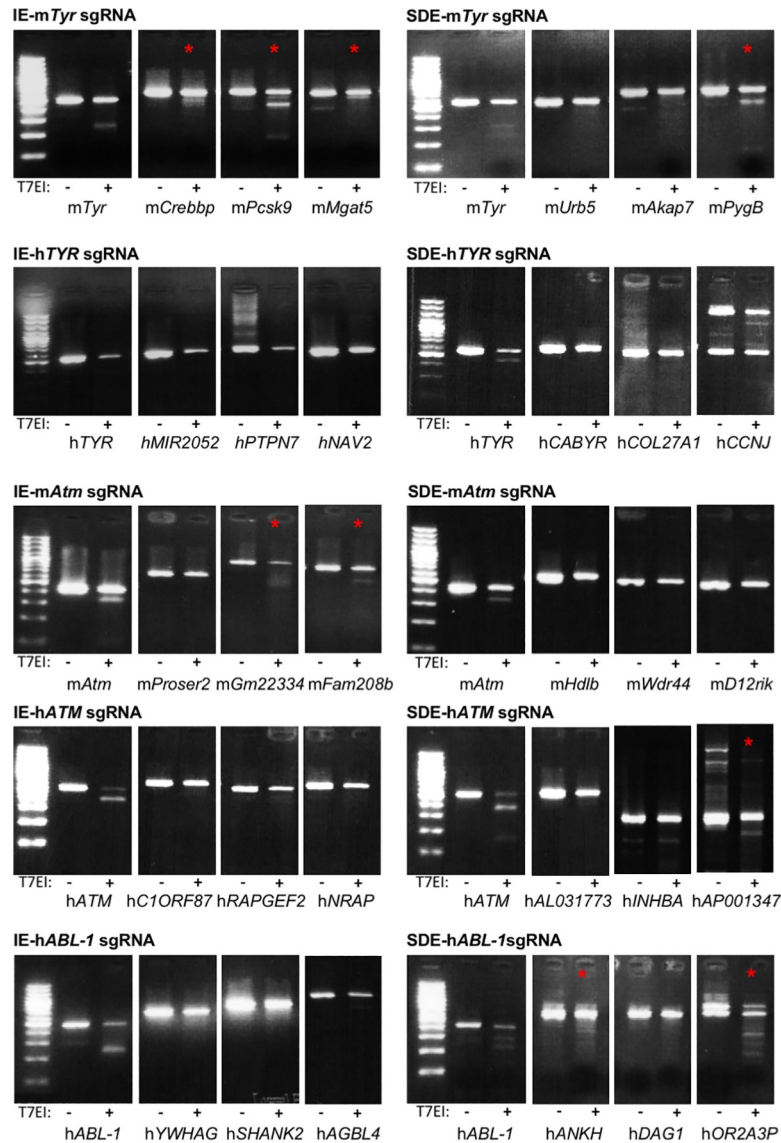


**Fig 8. Functional analysis of *BCR-ABL-1* in CRISPR/Cas9 edited K562 cells.** (A) Flow cytometry analysis of annexin V expression and cell cycle of K562-edited cells. SDE-hABL-1sgRNA trigger a higher number of apoptotic cells than IE-hABL-1sgRNA and control cells after electroporation with the empty vector. (B) The DNA content of the cells edited with SDE sgRNA gave 10% higher levels than IE-edited cells (45.3% vs. 34.5%). (C) The quantification of annexin V expression in K562-edited cells with SDE and IE hABL-1 sgRNAs showed a higher level of expression in SDE-hABL-1sgRNA edited cells (568,2 mfi) than in IE-hABL-1sgRNA-edited cells (475.5 mfi). Graph shows results from three independent experiments. \*\*\*,  $p < 0.001$ .

<https://doi.org/10.1371/journal.pone.0216674.g008>

mutations. These mutations can generate knockout alleles when CRISPR/Cas9 is directed at coding sequences, but due to the variable size of NHEJ-induced indels, generating a full KO in one step cannot always be achieved at high frequency. This could be especially critical for gene therapy approaches. If there is an acceptable degree of efficiency of delivery of CRISPR/Cas9 reagents to the target cell, the key step for success lies in the effectiveness of a specific sgRNA at knocking out the oncogene. In this context, the null effect could be increased by sgRNAs targeting the exon SD boundaries. Following this strategy, the generation of null alleles could be increased in two independent ways: by the probabilities of producing a frameshift mutation and/or breaking the canonical pre-mRNA splicing. In the present work we have demonstrated that knockout efficiency can be increased using sgRNAs targeting the exon splice donor area. The study considered the predicted informatic score (most guides with a score of  $> 75$ ) and the cut-site of the sgRNAs. It is important to note that for SDE-sgRNAs we chose PAMs to trigger DSBs inside the coding sequence that were located no further than five nucleotides from the end of the exon.

We noted that most of the mutant alleles produced in our assays in the Baf3 and k562 cell lines correspond to small indels, indicating that the DSB is repaired by blunt-end ligation independently of sequence homology, the classic nonhomologous end joining (C-NHEJ) mechanism[7]. NGS corroborated the Sanger sequences detected and exposed new mutant alleles that are likely to be little-represented in the edited cell line. As expected, NGS and Sanger



Off-target	IE-sgRNA	SDE-sgRNA
No edited	20	21
Edited	5	4

Chi-square test P=0.751 n.s.

**Fig 9. Off-targets analysis of sgRNAs.** Surveyor analysis of the top 5 predicted off-targets for each sgRNA used. Panel shows amplified sequence of target and 3 representative off-targets, non-treated and treated with T7 endonuclease I. Digestion reveals genome edition (red asterisk) when the off-target sequence carries some mutations. Table shows overall results from all off-targets analyzed. No differences were observed in number of edited off-targets by IE-sgRNAs compared with SDE-sgRNAs (Chi-square test P = 0.751 n.s.).

<https://doi.org/10.1371/journal.pone.0216674.g009>

sequencing highlighted the same alleles in *in vivo* assays of mouse zygotes, grown to blast or of mice born from them. *In silico* analysis of these mutant alleles revealed a full efficiency of the null effect in SDE-sgRNA compared with IE-sgRNA. When an IE-sgRNA was used, mutant alleles with mutations preserving the reading frame were detected. To corroborate the *in silico*

findings we Sanger-sequenced all mice born in both groups. Excluding unmutated mice, we detected color mice born from microinjected zygotes with IE-sgRNA with indels in one or more alleles. It is of particular note that we observed color mice with both alleles mutated, one of them with a frameshift mutation and the other with a mutation, indicating that some induced indels are not able to generate a frameshift mutation. By contrast, when we used a *Tyr* SDE-sgRNA, we detected albino or mosaic mice featuring one allele with a frameshift mutation and another with a mutation but a destroyed splice-donor site. This result demonstrates the higher null efficiency when an SDE-sgRNA is used. To determine whether this effect can be reproduced in another locus we employed the same assay but targeting the *ATM* and *ABL* loci. A similar result was obtained in both loci in human and mouse cell lines. Western blot analysis in cell clones from both groups corroborated the NGS and the results of their *in silico* analysis. More importantly, this approach can be efficiently used to abrogate oncogene expression. When a cancer cell is the target, a delivery strategy that can result in the expression of Cas9 and an oncogene-specific sgRNA in all infected cells is desirable. This is especially critical for *in vitro* gene therapy where the expansion processes of a selected edited cell are not available. Similarly, it is crucial for *in vivo* approaches in cancer therapies based on disrupting a driver oncogene. If the efficiency of delivery of CRISPR/Cas9 reagents to the cancer cell is acceptable, the key step for success lies in the effectiveness of a specific sgRNA at knocking out the oncogene. In most of these cases, the designs are based solely on off-target criteria. However, for those cases in which cellular selection is not an option and only one sgRNA can be used, the null effect could be increased with an sgRNA targeting the exon boundary. Various strategies at different molecular levels[24] have been employed to treat malignant diseases in recent decades, such as specific drug inhibitors acting at the protein level, gene suppression therapies at the mRNA level, and genome-editing nucleases at the DNA level. CRISPR/Cas9 works has the advantage of providing permanent and full gene knockout, and following this strategy, we abrogated p210 (BCR/ABLp210) oncoprotein expression in the K562 cell line. Using this approach, pools of K562 edited cells electroporated with SDE-sgRNAs or IE-sgRNA were studied. The loss of p210 expression in K562 cells with SDE-sgRNA resulted in a significant increase in apoptosis levels. Thus, this strategy could be adopted for gene therapy in cases for which cell selection is not an option and the delivery Cas9 vector only allows the accommodation of one sgRNA.

## Conclusions

Genome-editing nucleases, like the popular CRISPR/Cas9, enable knockout cell lines and null zygotes to be generated by inducing site-specific DSBs within a genome. In most cases, when a DNA template is not present, the DSB is repaired by non-homologous end joining, resulting in small nucleotide insertions or deletions that can be used to construct knockout alleles. However, for several reasons, these mutations do not produce the desired null result in all cases, giving rise to a similar but functionally active protein. This undesirable effect could limit the efficiency of gene therapy strategies based on abrogating oncogene expression by CRISPR/Cas9 and should therefore be borne in mind. The use of an sgRNA-targeting splice donor site could improve the null result for *in vivo* gene therapies. This strategy could be adopted to abrogate *in vivo* the oncogenic activity involved in tumor maintenance.

## Material & methods

### Ethics statement

This study followed Spanish and European Union guidelines for animal experimentation (RD 1201/05, RD 53/2013 and 86/609/CEE respectively). The study was approved by Bioethics Committee of the University of Salamanca and Junta de Castilla y León, Spain (ref.000359).

## Cell lines and culture conditions

Baf/3 is a murine interleukin 3-dependent murine pro-B cell [25]. Baf/3 was maintained in Dulbecco's Modified Eagle's Medium (DMEM) (Life Technologies) supplemented with 10% fetal bovine serum (FBS) and 1% of penicillin/streptomycin (Life Technologies) and 10% of WEHI-3-conditioned medium, as a source of IL-3.

The human CML-derived cell lines K562 were purchased from Deutsche Sammlung von Mikroorganismen and Zellkulturen (DSMZ). K562 cells were cultured in RPMI 1640 medium (Life Technologies) supplemented with 10% FBS, and 1% penicillin/streptomycin (Life Technologies). All cell lines were incubated at 37°C in a 5% CO<sub>2</sub> atmosphere. The presence of mycoplasma was tested frequently in all cell lines with a MycoAlert kit (Lonza), using only mycoplasma-free cells in all the experiments carried out.

## CRISPR/Cas9 system design and sgRNA cloning

pX458 (Addgene plasmid # 48138) [26], which contains the coding sequence of Cas9 nuclease and GFP, and a cloning site for sgRNA sequence, was digested with BpiI (NEB). To clone the sgRNAs into the pX458 vector, two complementary oligos were designed for each sgRNA that included two 4-bp overhang sequences (S9 Table). The sgRNA sequences were designed with the web tool of the Spanish National Biotechnology Centre (CNB)-CSIC (<http://bioinfogp.cnb.csic.es/tools/breakingcas/>).

Two sgRNAs were designed for the mouse *Tyr* locus. One of them, IE-*mTyr*sgRNA, targets the exonic sequence in *Tyr* exon1, and the other, SDE-*mTyr*sgRNA, targets the exon1-intron1-2 junction. Two sgRNAs were designed to target homologous sequences in the human *TYR* locus: IE-*hTYR*sgRNA and SDE-*hTYR*sgRNA (Fig 1A).

In the same way, two sgRNAs against the mouse *Atm* locus (IE-*mAtm*sgRNA and SDE-*mAtm*sgRNA) and two sgRNAs against the human *ATM* locus (IE-*hATM*sgRNA and SDE-*hATM*sgRNA) were designed, one of each pair in the coding sequence of exon 10 (IE) and the other against the *ATM* exon10-intron10-11 splice donor exon (SDE) (Fig 1B).

Finally, two sgRNA against human *ABL-1* locus were designed: IE-*hABL-1*sgRNA, which targets the exon 6 coding sequence, and SDE-*hABL-1*sgRNA, which targets the exon 4 splice donor sequence (Fig 1C).

The two complementary oligos used to conform each sgRNA (S9 Table) were denatured at 95°C for 5 min, ramp-cooled to 25°C over 45 min to allow annealing, and finally ligated with the linearized pX458. 2 µl of the ligation reaction were used to transform competent cells, and single colonies were expanded using a QIAprep spin Maxiprep Kit (Qiagen) before plasmid extraction. The correct insertion of the sgRNA sequences was confirmed by Sanger sequencing.

## In vitro cell electroporation

Mouse Baf/3 and human K562 cells were electroporated with pX458 containing sgRNAs against the *Tyr* and *ATM* loci, respectively, using Amaxa Nucleofector II (Lonza). 2 x 10<sup>6</sup> Baf/3 mouse cells were electroporated with 15 µg of plasmid in 100 µl of electroporation buffer (5 mM KCl; 15 mM MgCl<sub>2</sub>; 120 mM Na<sub>2</sub>HPO<sub>4</sub>/NaH<sub>2</sub>PO<sub>4</sub> pH7.2; 25 mM sodium succinate; 25 mM manitol) [27] using program X001, while 1 x 10<sup>6</sup> k562 cells were electroporated with 10 µg of plasmid using program T016. 24 hours after electroporation, GFP-positive cells were sorted by fluorescence-activated cell sorting (FACS) using FACS-Aria (BD Bioscience). 72 hours post-electroporation, the genome editing of the cells was analyzed.

## Sequencing of sgRNA targets sites

Genomic DNA from cells was extracted using the QIAamp DNA Micro Kit (Qiagen) following the manufacturer's protocol. To amplify the different target regions of human and mouse *TYR* and *ATM* genes, and human *ABL-1*, PCR was performed with the oligos described in [S10 Table](#). Genomic DNA from single blastocyst-staged embryo was extracted in 10  $\mu$ l of lysis buffer (50 mM KCL, 10 mM Tris-HCL pH 8.5, 0.1% Triton x-100, and 4 mg/ml of proteinase K) at 55°C overnight, then heated at 95°C for 10 min. 2  $\mu$ l of this DNA solution was used as a template for two rounds of PCR (30 cycles + 20 cycles) to amplify the target sequences using a specific primer for each region ([S11 Table](#)).

PCR products were purified using a High Pure PCR Product Purification Kit (Roche) and sequenced by the Sanger method using forward and reverse PCR primers.

The editing efficiency of the sgRNAs and the mutations potentially induced were assessed using Tracking of Indels by Decomposition (TIDE) software (<https://tide-calculator.nki.nl>; Netherlands Cancer Institute), which only required two Sanger sequencing runs from wild-type cells and mutated cells.

To specifically identify the different generated mutations, Next Generation Sequencing (NGS) technology was employed with the same Sanger primers with the corresponding adapters added, to read each edited sequence individually.

The purified amplicons were mixed in equimolar ratios according to the number of molecules and diluted to a final concentration of 0.2 ng/ $\mu$ l. The indexed paired-end library was prepared with a Nextera XT DNA Sample Preparation Kit (Illumina) and sequenced using an Illumina platform (NextSeq or MiSeq, 300 cycles). A median per base coverage of 27,538 reads (range 2096–88,976) was achieved. To call the sequence variants, an in-house bioinformatics pipeline was established. Sequencing reads were aligned to the mouse reference sequence genome (mm9) using bwa-0.7.12 software, and variant calling was performed with VarScan v2.4. To visualize read alignment and confirm the variant calls, Integrative Genomics Viewer version 2.3.26 (IGV, Broad Institute, MA) was used.

## Flow cytometry analysis and cell sorting of single-edited cell-derived clone

72 hours after sgRNA electroporation of K562 and Baf/3 cells, GFP-positive cells were selected by fluorescence-activated cell sorting (FACS) using FACS Aria (BD Biosciences), establishing the edited K562 and Baf/3 cell pool lines. For K562, single cells were seeded in 96-well plates by FACS, establishing six random single-cell-derived clones for both *ATM* sgRNAs, and used to analyze ATM protein expression. Six clones derived from cells electroporated with empty vector were used as controls.

## Western blotting

ATM protein expression was assessed by SDS-PAGE and western blot using a rabbit anti-ATM antibody (1:1000; 2873S; Cell Signaling). Horseradish peroxidase-conjugated  $\alpha$ -rabbit antibody (1:5000; 7074S; Cell Signaling) was used as a secondary antibody. Antibodies were detected using ECL Western Blotting Detection Reagents (RPN2209, GE Healthcare). The expression of vinculin (rabbit anti-vinculin; 1:1000; 4650S; Cell Signaling) was used as a loading control.

## *In vitro* transcription of CRISPR/Cas9 system components, animals and embryo microinjection

All sgRNA sequences were PCR-amplified from px458-based vector with primers carrying the T7 RNA polymerase promoter at the 5' ends ([S11 Table](#)), and after column purification

(Roche) the resulting PCR was used as a template for T7 RNA polymerase transcription *in vitro* (MEGAscript T7 Transcription Kit, Thermo Fisher).

The Cas9 nuclease ORF, including NLS, was also PCR-amplified with primers carrying the T7 RNA polymerase promoter at the 5' ends (S11 Table). The PCR product was purified and used as a template for *in vitro* transcription, 5' capping (mMESSAGE mMACHINE T7 Transcription Kit, Thermo Fisher), and 3' poly(A) tailing (Poly(A) Tailing Kit, Thermo Fisher). Transcription products were purified with RNeasy Mini Kit (Qiagen) and eluted in nuclease-free EmbryoMax microinjection buffer (Millipore).

One-cell-staged embryos from superovulated C57BL/6J or B6/CBA hybrid females were harvested and microinjected with 20 ng/ $\mu$ l of sgRNA and 20 ng/ $\mu$ l of Cas9 mRNA into the cytoplasm and pronucleus. Embryo donor mice were euthanized by cervical dislocation and were given humanitarian care in accordance with bioethical committee of University of Salamanca (ref. 000359) and Spanish and European Union guidelines for animal experimentation.

### Apoptosis and cell cycle analysis

Apoptosis was measured by flow cytometry with an annexin V-Dy634 apoptosis detection kit (ANXVVKDY, Immunostep) following the manufacturer's instructions. Briefly,  $5 \times 10^5$  cells were collected and washed twice in PBS, and labeled with annexin V-DY-634 and non-vital dye propidium iodide (PI), allowing the discrimination of living-intact cells (annexin-negative, PI-negative), early apoptotic cells (annexin-positive, PI-negative) and late apoptotic or necrotic cells (annexin-positive, PI-positive). In parallel, cell distribution in the cell cycle phase was also analyzed by measuring DNA content (PI labeling after cell permeabilization). Plots show results of a representative experiment from three independent replicates.

### Off-targets analysis

Predicted top 5 off-targets were analyzed by the T7 endonuclease I (T7EI) mismatch cleavage assay following manufacturer's indications (Integrated DNA Technologies) [28]. Target DNA sequences were amplified by PCR using specific oligonucleotides (S12 Table). To form the heteroduplex complexes, PCR products were denatured 95°C for 10 minutes, followed by temperature ramp (95–85°C, -2°C/sec and 85–25°C, 0.3°C/sec). The heteroduplex products were incubated with T7EI 1 hour at 37°C and visualized in 2% agarose gel.

### Statistical analysis

Statistical analysis of annexin V expression was performed using GraphPad Prism version 6.00 for Mac OS X, (GraphPad Software, La Jolla California USA, [www.graphpad.com](http://www.graphpad.com)). Experimental results were expressed as median  $\pm$  standard error (SEM). Nonparametric variables were analyzed using Kruskal-Wallis followed by Dunn's multiple comparisons test. Values with  $p < 0.001$  (indicated by three asterisks) were considered to be statistically significant. Chi-square test was performed to analyze the difference obtained in off-target analysis.

### Supporting information

**S1 Table. *In vitro* genome editing of the mouse *Tyr* locus using sgRNA against exon coding sequence (IE) and the coding splice-donor exon (SDE) sequence.** NGS analysis of allelic variants induced in Baf/3 mouse cells. (DOCX)

**S2 Table. *In vitro* genomic edition of human *TYR* locus using sgRNA against exon coding sequence (IE) and coding SDE sequence.** NGS analysis of allelic variants induced in K562

human cells.  
(DOCX)

**S3 Table. *In vitro* genome editing of the human *ATM* locus using sgRNA against the exon coding sequence (IE) and the coding SDE sequence.** NGS analysis of allelic variants induced in K562 human cells.

(DOCX)

**S4 Table. *In vitro* genome editing of the mouse *Atm* locus using sgRNA against the exon coding sequence (IE) and the coding SDE sequence.** NGS analysis of allelic variants induced in Baf/3 mouse cells.

(DOCX)

**S5 Table. NGS analysis of *ATM* allelic variants induced in human K562 single-edited cell-derived clones.**

(DOCX)

**S6 Table. *In vivo* genome editing of *Tyr* locus in mouse embryos using sgRNA against the coding sequence (IE) and the SDE sequence.** NGS analysis of allelic variants induced in microinjected mouse blastocysts.

(DOCX)

**S7 Table. *In vivo* genome editing of *Tyr* locus in mice using sgRNA against the coding sequence (IE) and the coding SDE sequence.** Observed phenotype and Sanger analysis of allelic variants induced in mice born after CRISPR/Cas9 system microinjection.

(DOCX)

**S8 Table. *In vitro* genome editing of the human *ABL-1* locus using sgRNA against the exon coding sequence (IE) and the coding SDE sequence.** NGS analysis of allelic variants induced in K562 cells.

(DOCX)

**S9 Table. Oligos designed for each sgRNA.**

(DOCX)

**S10 Table. Oligos used for target genome sequence amplification.**

(DOCX)

**S11 Table. Oligos used for *in vitro* transcription of sgRNA and Cas9 mRNA.**

(DOCX)

**S12 Table. Oligos used for off-target genome sequence amplification.**

(DOCX)

## Acknowledgments

The authors wish to express their sincere thanks to Dionisio Martín Zanca, Alberto Pendás (Spanish Research Council, CSIC), for their technical assistance and contribution to our CRISPR/Cas9 studies; Servicio de Citometría, Servicio de Experimentación Animal (University of Salamanca) and Servicio de Secuenciación (IBMCC) for their technical assistance.

## Author Contributions

**Conceptualization:** Ignacio García-Tuñón, Manuel Sánchez-Martín.

**Formal analysis:** Jesús María Hernández-Sánchez, Marta Martín-Izquierdo.

**Funding acquisition:** Jesús María Hernández-Rivas.

**Investigation:** Ignacio García-Tuñón, Verónica Alonso-Pérez, Elena Vuelta, Sandra Pérez-Ramos.

**Methodology:** Ignacio García-Tuñón, Verónica Alonso-Pérez, Elena Vuelta, Sandra Pérez-Ramos, María Herrero, Lucía Méndez, Jesús María Hernández-Sánchez, Marta Martín-Izquierdo.

**Resources:** Raquel Saldaña, Julián Sevilla, Fermín Sánchez- Guijo.

**Supervision:** Manuel Sánchez-Martín.

**Visualization:** Manuel Sánchez-Martín.

**Writing – original draft:** Ignacio García-Tuñón, Manuel Sánchez-Martín.

**Writing – review & editing:** Ignacio García-Tuñón, Manuel Sánchez-Martín.

## References

1. Gaj T, Gersbach CA, Barbas 3rd CF. ZFN, TALEN, and CRISPR/Cas-based methods for genome engineering. *Trends Biotechnol.* 2013/05/15. 2013; 31: 397–405. <https://doi.org/10.1016/j.tibtech.2013.04.004> PMID: 23664777
2. Grimm D, Kay MA. RNAi and gene therapy: a mutual attraction. *Hematol Am Soc Hematol Educ Progr.* 2007/11/21. 2007; 473–481. <https://doi.org/10.1182/asheducation-2007.1.473> PMID: 18024667
3. Bobbin ML, Rossi JJ. RNA Interference (RNAi)-Based Therapeutics: Delivering on the Promise? *Annu Rev Pharmacol Toxicol.* 2016/01/08. 2016; 56: 103–122. <https://doi.org/10.1146/annurev-pharmtox-010715-103633> PMID: 26738473
4. Porteus M. Genome Editing: A New Approach to Human Therapeutics. *Annu Rev Pharmacol Toxicol.* 2015/11/14. 2016; 56: 163–190. <https://doi.org/10.1146/annurev-pharmtox-010814-124454> PMID: 26566154
5. Garcia-Tunon I, Hernandez-Sanchez M, Ordonez JL, Alonso-Perez V, Alamo-Quijada M, Benito R, et al. The CRISPR/Cas9 system efficiently reverts the tumorigenic ability of BCR/ABL in vitro and in a xenograft model of chronic myeloid leukemia. *Oncotarget.* 2017; <https://doi.org/10.18632/oncotarget.15215> PMID: 28212528
6. Jinek M, Chylinski K, Fonfara I, Hauer M, Doudna JA, Charpentier E. A programmable dual-RNA-guided DNA endonuclease in adaptive bacterial immunity. *Science (80-).* 2012; 337: 816–821. <https://doi.org/10.1126/science.1225829> PMID: 22745249
7. Ceccaldi R, Rondinelli B, D'Andrea AD. Repair Pathway Choices and Consequences at the Double-Strand Break. *Trends Cell Biol.* 2015/10/07. 2016; 26: 52–64. <https://doi.org/10.1016/j.tcb.2015.07.009> PMID: 26437586
8. Haapaniemi E, Botla S, Persson J, Schmierer B, Taipale J. CRISPR-Cas9 genome editing induces a p53-mediated DNA damage response. *Nat Med.* 2018/06/13. 2018; 24: 927–930. <https://doi.org/10.1038/s41591-018-0049-z> PMID: 29892067
9. Kosicki M, Tomberg K, Bradley A. Repair of double-strand breaks induced by CRISPR-Cas9 leads to large deletions and complex rearrangements. *Nat Biotechnol.* 2018/07/17. 2018; 36: 765–771. <https://doi.org/10.1038/nbt.4192> PMID: 30010673
10. Kotterman MA, Schaffer D V. Engineering adeno-associated viruses for clinical gene therapy. *Nat Rev Genet.* 2014; 15: 445–451. <https://doi.org/10.1038/nrg3742> PMID: 24840552
11. Kim E, Koo T, Park SW, Kim D, Kim K, Cho HY, et al. In vivo genome editing with a small Cas9 orthologue derived from *Campylobacter jejuni*. *Nat Commun.* 2017; 8: 14500. <https://doi.org/10.1038/ncomms14500> PMID: 28220790
12. Graham DB, Root DE. Resources for the design of CRISPR gene editing experiments. *Genome Biol.* 2015; 16: 260. <https://doi.org/10.1186/s13059-015-0823-x> PMID: 26612492
13. Sanchez-Garcia I. Consequences of chromosomal abnormalities in tumor development. *Annu Rev Genet.* 1997/01/01. 1997; 31: 429–453. <https://doi.org/10.1146/annurev.genet.31.1.429> PMID: 9442903

14. Perez-Mancera PA, Sanchez-Garcia I. Understanding mesenchymal cancer: the liposarcoma-associated FUS-DDIT3 fusion gene as a model. *Semin Cancer Biol.* 2005/04/14. 2005; 15: 206–214. <https://doi.org/10.1016/j.semcancer.2005.01.006> PMID: 15826835
15. Wassef M, Luscan A, Battistella A, Le Corre S, Li H, Wallace MR, et al. Versatile and precise gene-targeting strategies for functional studies in mammalian cell lines. *Methods.* 2017; 121–122: 45–54. <https://doi.org/10.1016/j.ymeth.2017.05.003> PMID: 28499832
16. Krawczak M, Reiss J, Cooper DN. The mutational spectrum of single base-pair substitutions in mRNA splice junctions of human genes: causes and consequences. *Hum Genet.* 1992/09/01. 1992; 90: 41–54. PMID: 1427786
17. Treisman R, Proudfoot NJ, Shander M, Maniatis T. A single-base change at a splice site in a beta 0-thalassaemic gene causes abnormal RNA splicing. *Cell.* 1982/07/01. 1982; 29: 903–911. PMID: 7151176
18. Treisman R, Orkin SH, Maniatis T. Specific transcription and RNA splicing defects in five cloned beta-thalassaemia genes. *Nature.* 1983; 302: 591–596. Available: <https://www.ncbi.nlm.nih.gov/pubmed/6188062> PMID: 6188062
19. Camats N, Pandey A V, Fernandez-Cancio M, Fernandez JM, Ortega AM, Udhane S, et al. STAR splicing mutations cause the severe phenotype of lipoid congenital adrenal hyperplasia: insights from a novel splice mutation and review of reported cases. *Clin Endocrinol.* 2014; 80: 191–199. <https://doi.org/10.1111/cen.12293> PMID: 23859637
20. Matsuda D, Sato H, Maquat LE. Chapter 9. Studying nonsense-mediated mRNA decay in mammalian cells. *Methods Enzym.* 2009/02/14. 2008; 449: 177–201. [https://doi.org/10.1016/s0076-6879\(08\)02409-9](https://doi.org/10.1016/s0076-6879(08)02409-9)
21. Elsayed LEO, Mohammed IN, Hamed AAA, Elseed MA, Salih MAM, Yahia A, et al. Case report of a novel homozygous splice site mutation in PLA2G6 gene causing infantile neuroaxonal dystrophy in a Sudanese family. *BMC Med Genet.* 2018/05/10. 2018; 19: 72. <https://doi.org/10.1186/s12881-018-0592-y> PMID: 29739362
22. Liu G, Wang X, Qin M, Sun L, Zhu J. A Novel Splicing Mutation of Ectodysplasin A Gene Responsible for Hypohidrotic Ectodermal Dysplasia. *Oral Dis.* 2018/04/21. 2018; <https://doi.org/10.1111/odi.12874> PMID: 29676859
23. Wood-Trageser MA, Gurbuz F, Yatsenko SA, Jeffries EP, Kotan LD, Surti U, et al. MCM9 mutations are associated with ovarian failure, short stature, and chromosomal instability. *Am J Hum Genet.* 2014/12/07. 2014; 95: 754–762. <https://doi.org/10.1016/j.ajhg.2014.11.002> PMID: 25480036
24. García-Tuñón I, Vuelta E, Pérez-Ramos S, Hernández-Rivas JM, Méndez L, Herrero M, et al. CRISPR-ERA for Switching Off (Onco) Genes. In: Singh Aditi, editor. *Modulating Gene Expression—Abridging the RNAi and CRISPR-Cas9 Technologies.* IntechOpen; 2018. <https://doi.org/10.5772/intechopen.80245>
25. Palacios R, Steinmetz M. II-3-dependent mouse clones that express B-220 surface antigen, contain Ig genes in germ-line configuration, and generate B lymphocytes in vivo. *Cell.* 1985/07/01. 1985; 41: 727–734. PMID: 3924409
26. Ran FA, Hsu PD, Wright J, Agarwala V, Scott DA, Zhang F. Genome engineering using the CRISPR-Cas9 system. *Nat Protoc.* 2013/10/26. 2013; 8: 2281–2308. <https://doi.org/10.1038/nprot.2013.143> PMID: 24157548
27. Chicaybam L, Barcelos C, Peixoto B, Carneiro M, Limia CG, Redondo P, et al. An Efficient Electroporation Protocol for the Genetic Modification of Mammalian Cells. *Front Bioeng Biotechnol.* 2016; 4: 99. <https://doi.org/10.3389/fbioe.2016.00099> PMID: 28168187
28. Vouillot L, Thélie A, Pollet N. Comparison of T7E1 and surveyor mismatch cleavage assays to detect mutations triggered by engineered nucleases. *G3 (Bethesda).* 2015; 5: 407–15. <https://doi.org/10.1534/g3.114.015834> PMID: 25566793